



HAL
open science

In-Situ Fabrication of aligned equiaxed Materials by High Magnetic Field during directional solidification

Du Dafan, Li Xi, Yves Fautrelle, Annie Gagnoud, Zhongming Ren, Deng Kang

► **To cite this version:**

Du Dafan, Li Xi, Yves Fautrelle, Annie Gagnoud, Zhongming Ren, et al.. In-Situ Fabrication of aligned equiaxed Materials by High Magnetic Field during directional solidification. 8th International Conference on Electromagnetic Processing of Materials, Oct 2015, Cannes, France. hal-01331649

HAL Id: hal-01331649

<https://hal.science/hal-01331649>

Submitted on 14 Jun 2016

HAL is a multi-disciplinary open access archive for the deposit and dissemination of scientific research documents, whether they are published or not. The documents may come from teaching and research institutions in France or abroad, or from public or private research centers.

L'archive ouverte pluridisciplinaire **HAL**, est destinée au dépôt et à la diffusion de documents scientifiques de niveau recherche, publiés ou non, émanant des établissements d'enseignement et de recherche français ou étrangers, des laboratoires publics ou privés.

In-Situ Fabrication of aligned equiaxed Materials by High Magnetic Field during directional solidification

Du Dafan¹, Li Xi^{1,2}, Yves Fautrelle^{2,3}, Annie Gagnoud^{2,3}, Zhongming Ren¹, Deng Kang¹

¹ Department of Material Science and Engineering, Shanghai University, Shanghai, 200072, P. R. China

² Univ. Grenoble Alpes, SIMAP, F-38000 Grenoble, France

³ CNRS, SIMAP, F-38000 Grenoble, France

Corresponding author: lx_net@sina.com-Li Xi

Abstract

The application of a high magnetic field was capable of inducing the formation of aligned equiaxed grains during directional solidification. The alignment and refinement of equiaxed grains were enhanced as the magnetic field intensity increased. Further, the thermoelectric power difference at the liquid/solid interface in four alloys was measured *in-situ* during directional solidification. The formation of aligned equiaxed grains under the magnetic field should be attributed to the combined action of thermoelectric magnetic force and magnetization force.

Key words : Equiaxed grains; Alignment; High magnetic field; Directional solidification.

Introduction

Effect of external conditions on the dendrite growth is always a research hotspot [1-5]. The magnetic field (i.e., static, rotating and traveling magnetic fields) as a special external condition has been applied during the dendrite growth. It has been demonstrated that the static magnetic field enhanced the dendrite growth, and the rotating and traveling magnetic fields destroyed the dendrite growth [6-9]. Recently, a high magnetic field has widely been applied during solidification processes [10-13]. It has been found that the application of a high magnetic field has caused the branch and break of the dendrites in the Al-Cu alloy at a lower growth speed [13]. The present work extends the previous works and investigates the influence of a high magnetic field on the dendrite growth in several alloys during directional solidification in detail using electron backscatter diffraction (EBSD). The results indicated that the application of a high magnetic field caused the columnar-to-equiaxed transition (CET) and the formation of aligned equiaxed grains during directional solidification. The TE (Thermoelectric) power difference at the liquid/solid interface in the alloys was measured *in-situ*. The results indicated that there indeed existed a TE power difference at the liquid/solid interface and the values of the Seebeck signal were on the order of 1 - 10 μV . The numerical results revealed that the TE magnetic force produced on the tip of the dendrite induced a moment during directional solidification. The formation of aligned equiaxed grains during directional solidification under the magnetic field should be attributed to the combined action of TE magnetic force and magnetization force.

Experimental

Al-7wt%Si alloy, Sn-20wt%Pb alloy were solidified directionally under an axial high magnetic field. Cast samples were enveloped in tubes of high-purity corundum with an inner diameter of 3 mm and length of 200 mm. The schematic view of the directional solidification apparatus under an axial strong magnetic field is shown in Ref. [14], where the apparatus was described in detail. The specimen contained in a corundum crucible was melted and directionally solidified in the Bridgman apparatus by pulling the crucible assembly downwards at a constant growth speed by means of a synchronous motor. After 80 mm of steady-state growth of the specimen, the quenching experiment was performed by quickly withdrawing the crucible into the water-cooled cylinder containing liquid Ga-In-Sn metal. Microstructures were investigated by the electron backscatter diffraction (EBSD) in a high-resolution scanning electron microscope equipped with EDAX's OIM EBSD Analysis System.

Results and Discussion

Fig. 1(a) and Fig. 1(b) show the EBSD orientation map for the structures near the liquid/solid interface of the above two alloys without and with a 12 T magnetic field. It can be observed that the dendrites were typical columnar and aligned with their respective preferred growth directions along the solidification direction without magnetic field. However, the regular columnar dendrites were destroyed significantly and tended to transform into the equiaxed grains with application of magnetic field. Along with the CET, the equiaxed grains tended to be aligned with a certain crystal direction along the magnetic field. Fig. 1(c) and 1(d) shows corresponding pole figures for the longitudinal structures in Sn-20wt%Pb and Al-7wt%Si alloys under a 12 T magnetic field; the data indicate that the aligned equiaxed grains formed. Indeed, the β -Sn, and α -Al equiaxed grains tended to be oriented with the $\langle 100 \rangle$ - and $\langle 111 \rangle$ - crystal directions along the magnetic field, respectively.

Further, to study the alignment rule of the equiaxed grains during directional solidification under a high magnetic field,

the microstructures in directionally solidified Sn-20wt%Pb alloy under various magnetic fields were investigated in detail. Fig. 2 shows the EBSD orientation maps and corresponding inverse pole figures for the structures near the liquid/solid interface. The Sn columnar dendrite was observed to be aligned with its preferred growth direction (i.e., the $\langle 110 \rangle$ -crystal direction) along the solidification direction without magnetic field. However, when the high magnetic field was applied, along with the CET of the dendrite morphology, the volume fraction of aligned grains gradually increased as the magnetic field intensity increased. Moreover, the size of the equiaxed grains decreased as the magnetic field increased.

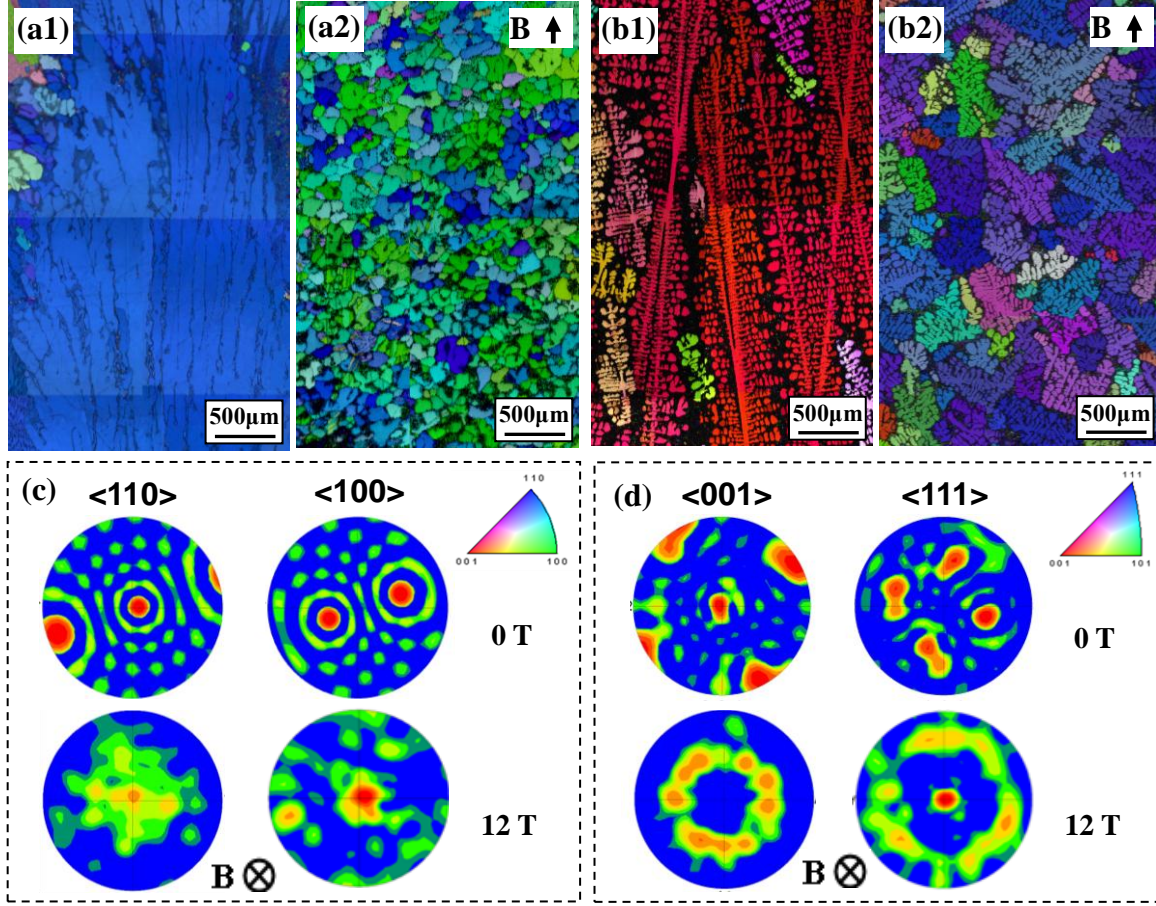


Fig. 1. EBSD orientation maps and corresponding pole figures for the longitudinal structure in directionally solidified alloys without and with a 12 T magnetic field: (a, c) Sn-20wt%Pb alloy, 1 $\mu\text{m/s}$; (b, d) Al-7wt%Si alloy, 80 $\mu\text{m/s}$.

As we know, a high magnetic field ($B > 1.0 \text{ T}$) is strong enough to damp the convections in a liquid. From this viewpoint, the application of a high magnetic field should enhance the formation of regular columnar dendrites. However, the above experimental results indicate that the magnetic field destroyed the formation of regular columnar dendrites. This behavior should be attributed to the generation of the stress on the solid under the magnetic field. Normally, the magnetization force and the thermoelectric (TE) magnetic force will be produced during directional solidification under the magnetic field. First, the TE magnetic force acting on the dendrites was investigated. Because of the Seebeck effects [15], an interdendritic TE current will form during directional solidification. The following approximation for the electric current density j_s in the solid was assumed [16]:

$$j_s = \frac{-\sigma_L \sigma_s f_L}{\sigma_L f_L + \sigma_s f_s} (S_s - S_L) G \quad (1)$$

where σ_L and σ_s and are the electrical conductivity of liquid and solid, respectively; f_L and f_s are the liquid and solid fractions, respectively; S_L and S_s are the TE powers of the liquid and solid, respectively; G is the temperature gradient. When an external magnetic field B is applied because the TE current J_{TE} cannot be everywhere parallel to B , the Lorentz forces $J_{TE} \times B$ (i.e., the TE magnetic force) will form in the dendrites:

$$F_s = \frac{-\sigma_L \sigma_s f_L}{\sigma_L f_L + \sigma_s f_s} (S_s - S_L) G B \quad (2)$$

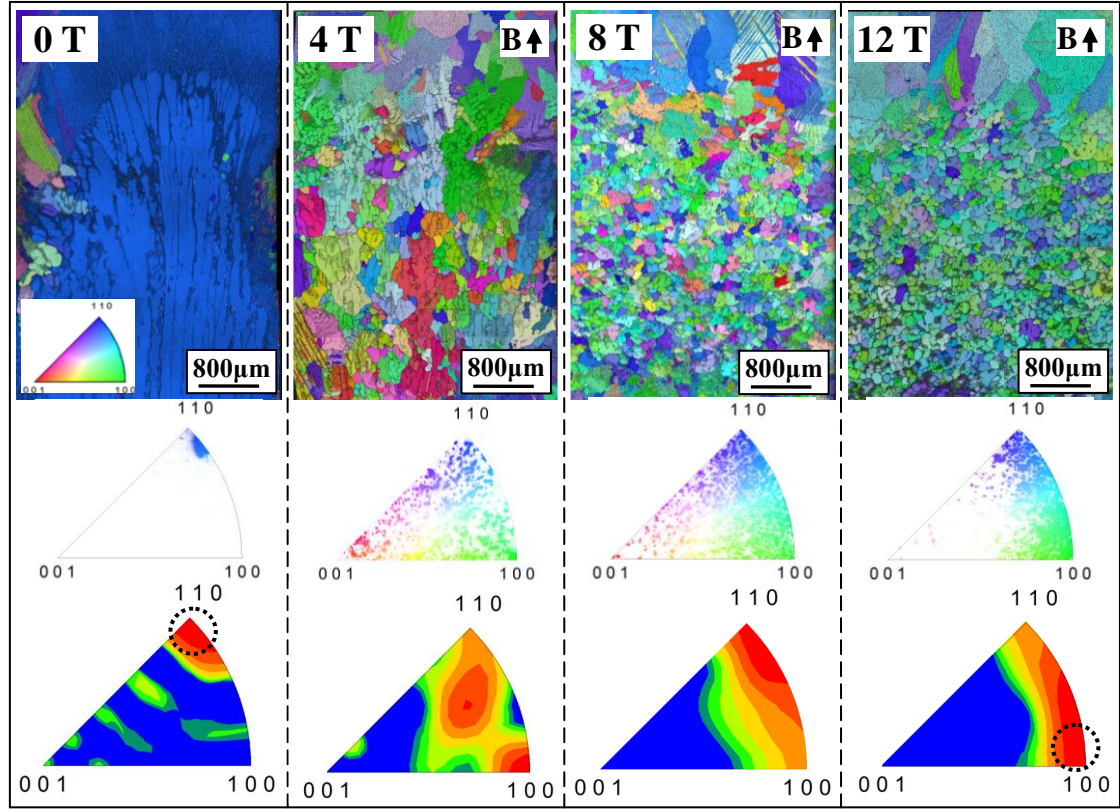


Fig. 2. EBSD orientation maps and corresponding pole figures for the structure near the liquid/solid interface in directionally solidified Sn-20wt%Pb alloy at a growth speed of $1 \mu\text{m/s}$ under various magnetic fields.

To investigate the distribution and amplitude of the TE magnetic force, the force near the liquid/solid interface was numerically simulated via the commercial software COMSOL Multiphysics (version 4.2.0.228). Fig. 3(a) shows the simulated TE magnetic force near the liquid/solid interface in directionally solidified Al-Cu alloy under an axial magnetic field. The TE magnetic force and moment acted on the tip of the dendrite when an axial magnetic field was applied. Further, to confirm the existence of a TE power difference at the liquid/solid interface ($\eta_{sl} = S_S - S_L$) during directional solidification, the Seebeck signals of four alloys were measured *in-situ*. The basic principle of the interfacial TE measurement using the Seebeck technique is schematically presented in Fig. 3(b). The details of the principle had been discussed in Refs. [17, 18]. Fig. 3(c) shows the Seebeck response obtained for the Al-7wt%Si and Sn-20wt%Pb alloys at a growth speed of $5 \mu\text{m/s}$. One can see that a plateau was obtained on the Seebeck curve to indicate the establishment of steady state, and then the signal decreased to a new steady state when the furnace translation was shut off. The magnitude of the signal drop, $E_s = (S_S - S_L)\Delta T$, corresponds directly to the effective liquid/solid TE power difference (η_{sl}). The above results indicate that there indeed existed a TE power difference at the liquid/solid interface during directional solidification of metal alloys. Moreover, from Eq. (2), it can be deduced that the TE magnetic force increases as the magnetic field intensity increases. Thus, when the TE magnetic force becomes strong enough to break the dendrite, the number of the equiaxed grains ahead of the columnar front increases. According to Hunt's mode [19], when the volume fraction of the equiaxed grains exceeds 0.49, the CET will occur. For an equiaxed grain exhibiting magnetic crystalline anisotropy, the easy magnetization axis of the equiaxed grain tends to rotate towards the magnetic field. As a consequence, the aligned equiaxed grains form during directional solidification under the magnetic field.

Conclusions

In summary, we can conclude the following:

1. The application of a high magnetic field caused the CET and the formation of the aligned equiaxed grains during directional solidification. The alignment and the refinement of the equiaxed grains were enhanced as the magnetic field intensity increased.
2. Seebeck thermoelectric force (E_s) at the liquid/solid interface in four alloys was measured *in-situ*, and the results indicated that the value of the Seebeck signal was on the order of 1-10 μV .
3. The formation of the aligned equiaxed grains during directional solidification under the magnetic field should be

attributed to the combined action of TE magnetic force and magnetization force.

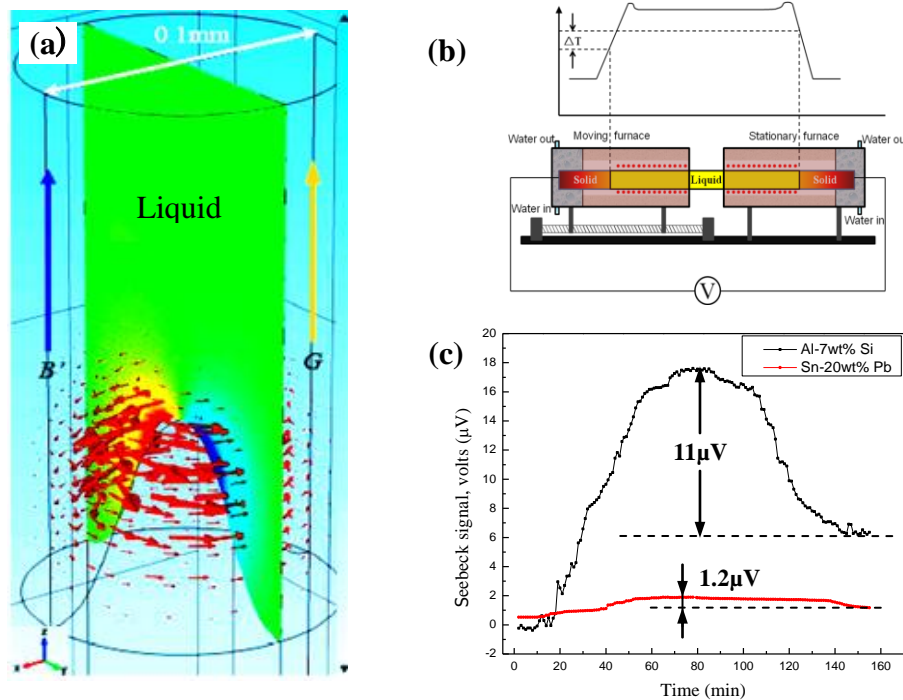


Fig. 3. Formation of aligned equiaxed grains during directional solidification under an axial high magnetic field: (a) Simulative TE current and magnetic force near the liquid/solid interface in 0.1 mm diameter geometry in directionally solidified Al-Cu alloy under an axial magnetic field; (b) Schematic diagram of the MEPHISTO apparatus; (c) Seebeck response obtained for the Al-7wt% Si and Sn-20wt% Pb alloys during directionally solidified at a growth speed of 5 $\mu\text{m/s}$.

Acknowledgements

This work is supported partly by European Space Agency through the BI-inter 09_473220, National Natural Science Foundation of China (Nos. 51271109, 51171106 and 2011CB610404) and the Program for Professor of Special Appointment (Eastern Scholar) at Shanghai Institutions of Higher Learning.

References

- [1] K. Murakami, T. Fujiyama, A. Koike and T. Okamoto (1983), *Acta Metall.* 31, 1425-1432.
- [2] K. Dragnevski, R.F. Cochrane and A.M. Mullis (2002), *Phys. Rev. Lett.* 89, 215502-1.
- [3] C. Vives (1996), *Metall. Mater. Trans. B* 27, 457-464.
- [4] B. Wei, D.M. Herlach, B. Feuerbacher and F. Sommer (1993), *Acta Metall.* 41, 1801-1809.
- [5] M. Wu and A. Ludwig (2009), *Acta Mater.* 57, 5621-5631.
- [6] B. Willers, S. Eckert, U. Michel and G. Zouhar (2005), *Mater. Sci. Eng. A* 402, 55-65.
- [7] C. Vives (1990), *Int. J. Heat Mass Trans.* 33, 2585-2598.
- [8] A.E. Ares and C.E. Schvezov (2000), *Metall. Mat. Trans. A* 31, 1611-1625.
- [9] D.R. Uhlmann, T.P. Seward and B. Chalmers (1996), *Trans. Met. Soc. AIME* 236, 527-530.
- [10] H. Yasuda, I. Ohnaka, Y. Yamamoto, A.S. Wismogroho, N. Takezawa and K. Kishio (2003), *Mater. Trans. JIM* 44, 2550-2554.
- [11] T. Liu, Q. Wang, A. Gao, C. Zhang, C.J. Wang and J.C. He (2007), *Scr. Mater.* 57, 992-995.
- [12] L. Li, Y.D. Zhang, C. Esling, H.X. Jiang, Z.H. Zhao, Y.B. Zuo and J.Z. Cui (2012), *J. Cryst. Growth* 339, 61-69.
- [13] X. Li, Y. Fautrelle and Z.M. Ren (2007), *Acta Mater.* 55, 5333-5347.
- [14] X. Li, Z.M. Ren and Y. Fautrelle (2006), *Acta Mater.* 54, 5349-5360.
- [15] J.J. Shercliff (1979), *Fluid Mech.* 91, 231-251.
- [16] P. Lehmann, R. Moreau, D. Camel and R. Bolcato (1998), *Acta Mater.* 46, 4067-4079.
- [17] J.J. Favier, J.P. Garandet, A. Rouzaud and D. Camel (1994), *J. Cryst. Growth* 140, 237-243.
- [18] S. Sen, B.K. Dhindaw, P.A. Curreri, P. Peters and W.F. Kaukler (1998), *J Cryst. Growth* 193, 692-700.
- [19] J.D. Hunt (1984), *Mater. Sci. Eng. A* 65, 75-83.